5th Australasian Congress on Applied Mechanics, ACAM 2007
10-12 December 2007, Brisbane, Australia

Optimum Shapes for Minimising Bond Stress in Scarf Repairs

Chun H. Wang[1] and Andrew J. Gunnion[2]

[1] *Air Vehicles Division, Defence Science and Technology Organisation,*
506 Lorimer Street, Fishermans Bend VIC 3207, Australia
[2] *Cooperative Research Centre for Advanced Composite Structures Ltd.,*
506 Lorimer Street, Fishermans Bend VIC 3207, Australia

Abstract: Bonded scarf repairs are used in composite structures when high strength recovery is needed or when there is a requirement for a flush surface to satisfy aerodynamic or stealth requirements. However, scarf repairs are complex to design and require the removal of significant parent structure, particularly for thick skins. In this investigation, analytical and numerical approaches have been developed to investigate whether an optimum repair shape for a known biaxial load can be determined. The results clearly demonstrate that the strength of a repaired panel can be improved by optimising both the initial damage cut-out shape and the scarf angle distribution.

Keywords: composite materials, optimum shapes, scarf repairs.

1 Introduction

Traditionally, the design of a scarf repair has been based on an equivalent 2-D joint approach, which simplifies the 3-D repair down to a 2-D joint oriented in the direction of maximum load. The designer then adopts the critical scarf angle determined from the 2-D joint analysis as the scarf angle of the repair, keeping the scarf angle constant in every direction. Depending on the loads experienced by the repaired structure, such a repair with constant scarf angle may be overly conservative in other directions, causing unnecessary removal of pristine material. This can be particularly significant for structures that are more highly stressed in one direction than any other. To minimise unnecessary material removal, it is advantageous to determine the optimum shape of scarf repairs for structures under an arbitrary bi-axial tension stress state.
This investigation proceeds as follows; existing design methods are reviewed; the general optimisation problem for a scarf repair is formulated; various optimum or near optimum solutions are explored; finally issues of practical application discussed and highlighted for future investigation.

2 Comparison of Current Shaping Methodologies

Three current approaches for determining the shape of a scarf repair are evaluated under assumptions of biaxial stress states. In this review, they will be referred to as the “maximum principal stress” (MPS) method, the “linear interpolation” (LI) method and the “radial stress” (RS) method.

2.1 Summary of Shaping Methodologies

A structural model of scarf repair can be represented by a flat panel with a circular cut-out to remove damage. The structure is subjected to a biaxial stress state with principal stresses being denoted as σ_x and σ_y, as shown in Figure 1. The maximum-principal-stress method considers a slice taken through the repair in-line with the direction of the maximum principal stress and then applies an equivalent 2-D joint analysis to calculate the necessary scarf angle (α). The scarf angle is then assumed to be constant in every direction around the scarf. The linear-interpolation method assumes that the scarf angle varies linearly with the radial angle between the two principal stress directions. The scarf angles at these two directions are determined using the respective equivalent 2-D joints. The radial-stress method applies the joint design along any radial slice, using the radial stress at each angle to determine the necessary scarf ratio using the following expression:

$$\alpha = \frac{1}{2}\sin^{-1}\left(\frac{2\tau_Y}{\sigma_r(\theta)}\right) \tag{1}$$

with the radial stress σ_r being given by $\sigma_r = \sigma_x \cos^2\theta + \sigma_y \sin^2\theta$.

2.2 Computational Assessment

To evaluate the aforementioned three methods, a scarf repair to a flat panel (thickness=*h*) subjected to biaxial stresses was selected for consideration, as shown in Figure 1. Finite element (FE) models of repairs pertinent to each method were analysed. To simplify the analysis, the parent structure and the repair patch were modelled as a homogenous, isotropic material with properties. This simplification significantly reduced the modelling and computational effort required. Although this simplification is known to influence the local stress state within the adhesive bondline, the influence is well documented and understood [1-4], making it relatively easy to transfer any design implications to the more complex scenario of a composite laminate. The boundary conditions, loads and material are such that the model symmetry can be exploited to further reduce the computational effort.

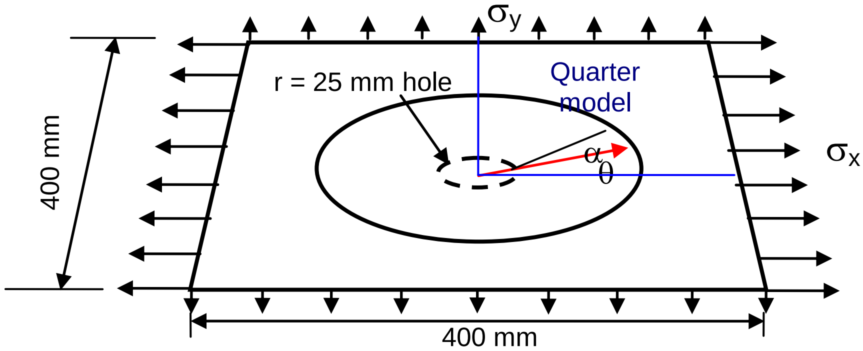

Figure 1. Panel and scarf repair under biaxial loading used to evaluate repair geometries

A adhesive failure criterion convenient for computation implementation was adopted,

$$\left(\frac{\tau}{\tau_{\max}}\right)^a + \left(\frac{\sigma_{peel}}{\sigma_n}\right)^b = 1\,. \tag{2}$$

where $\tau_{\max}$ and σ_n denote the maximum shear stress and the normal stress at the mid-plane of the adhesive layer. For the optimisation study, a failure criterion index (FCI) can be defined such that a value of greater than or equal to unity means that the adhesive has been stressed beyond failure,

$$FCI = \left(\frac{\tau}{\tau_{\max}}\right)^a + \left(\frac{\sigma_{peel}}{\sigma_n}\right)^b\,. \tag{3}$$

To evaluate the different repair schemes, FE analyses were carried out on the repairs designed using the MPSM, LIM and RSM approaches where $\sigma_x = 4\sigma_y$. An automated modelling tool was developed using Patran Command Language (PCL) within MSC.Patran to generate the scarf repair models. To ensure that the scarf angles remained representative of real repairs, the smallest scarf angle was constrained to 3º. Hence, the material allowables were determined such that the 3º scarf was the optimum scarf angle in the x-direction (θ = 0º). For this stress ratio and material adhesive properties, the optimum scarf angle in the y-direction (θ = 90º) was 12.4º. The resulting repair geometries are shown in Figure 2 with a circular damage cut-out radius of 25 mm. The linear static analyses was performed using MSC.Nastran. The exponents *a* and *b* are equal to 1.0 and 10.0, respectively.

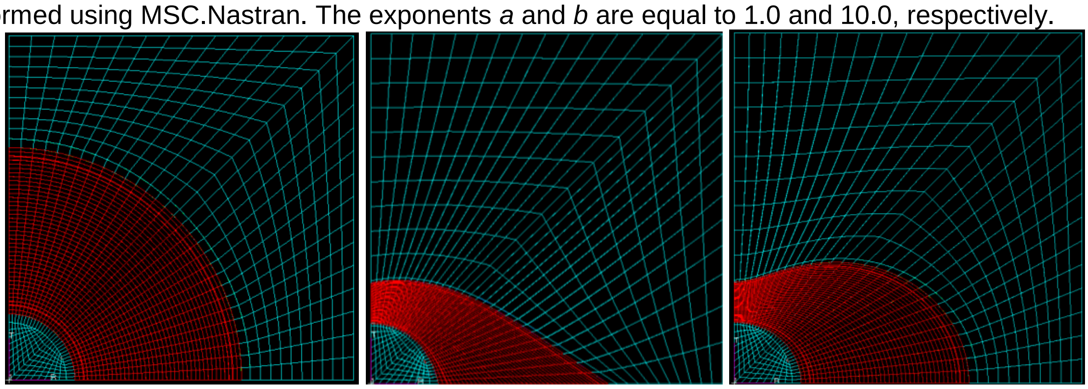

(a) (b) (c)

Figure 2. Scarf repair shapes determined using the (a) MPSM, (b) LIM and (c) RSM approaches

2.3 Results & Discussion

For each repair, the FCI along the bondline was calculated as a post-processing procedure in Patran and is compared in Figure 3. It can be seen that none of the design methods can be considered near-optimum, as they all result in significant variation in the FCI around the scarf surface. The MPSM and RSM approaches result in a scarf design that is overly conservative, resulting in excessive material removal, whilst the LIM method actually results in a non-conservative solution, as there is a significant region of the bondline with an FCI as high as 1.58.

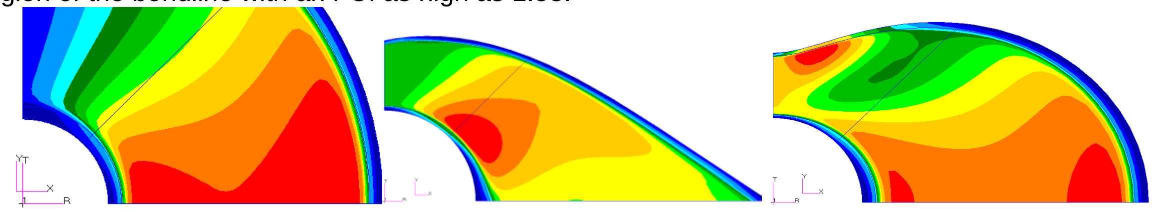

(a) (b) (c)

Figure 3. FCI results for the (a) MPSM (max. = 1.08) (b) LIM (max. = 1.58) and (c) RSM (max. = 1.12), demonstrating that none produce an optimum repair (common min.fringe value = 0.1)

3. Formulation of the Optimisation Problem

The non-uniformity of the stresses along the scarf bondline shown in Figure 3 would result in severe load-carrying penalties even for ductile adhesives, because the average shear stress in a composite repair remains below the adhesive's yield strength [4]. Therefore, it is possible to achieve higher joint strength by optimising the scarf shape so that the stress concentration is minimised. In essence, the present approach resembles the fully stressed design (optimisation approach of general structural synthesis [5]). The overall objective is to determine a surface with uniform failure index, within the limits of the parent structure, subject to a constant far-field biaxial stress state σ_x and σ_y. Denoting the scarf surface as,

$$Z = f(x,y), \text{ where } \quad z_{lower} \le Z \le z_{upper} \tag{4}$$

The plate-like structure is subjected to generalized plane stress,

$$[\sigma] = \begin{bmatrix} \sigma_{xx} & \tau_{xy} & 0 \\ \tau_{xy} & \sigma_{yy} & 0 \\ 0 & 0 & 0 \end{bmatrix}. \tag{5}$$

The surface normal at an arbitrary location is,

$$\vec{n} = \frac{-1}{\sqrt{1+(\partial f/\partial x)^2 + (\partial f/\partial y)^2}}\left(\frac{\partial f}{\partial x}\vec{i} + \frac{\partial f}{\partial y}\vec{j} - \vec{k}\right). \tag{6}$$

At an arbitrary point (x, y, z) on the scarf surface, the peel stress normal to scarf surface is

$$\sigma_n = \vec{n}\cdot[\sigma]\cdot\vec{n} \tag{7}$$

The maximum shear stress tangential to the scarf surface is

$$\tau_{\max} = \sqrt{\left\|[\sigma]\cdot\vec{n}\right\|^2 - \sigma_n^2} \tag{8}$$

Optimal scarf surface is defined as a surface on which the adhesive is equally critical, *i.e.*, the maximum shear stress and the peel stress satisfy FCI = 1. The optimization problem now reduces to solving a non-linear differential equation. It should be noted that the true optimal scarf surface may no longer be expressed by a single angle (α). In other words, the intersection between the optimal surface and radial plane (r_θ-z plane), shown schematically in Figure 4(a), may not be a straight line. To simplify the problem, it is assumed in this investigation that the scarf angle remains constant along any r_θ-z plane, as is illustrated in Figure 4(b). In this case, the scarf surface can be expressed as

$$Z = [r - r_0(\theta)]\tan\alpha(\theta), \quad r_0(\theta) < r < r_h(\theta), \tag{9}$$

where $r_0(\theta)$ and $r_h(\theta)$ denotes the intersection of the scarf with the lower plate surface ($z = 0$) and the upper plate surface ($z = h$). Now the optimization problem reduces to solving a non-linear differential equation for the unknown function $\alpha(\theta)$, for a given inner cut-out shape $r_0(\theta)$. The resulting equation is not amenable to explicit closed-form solutions, but can be solved using an iterative method.

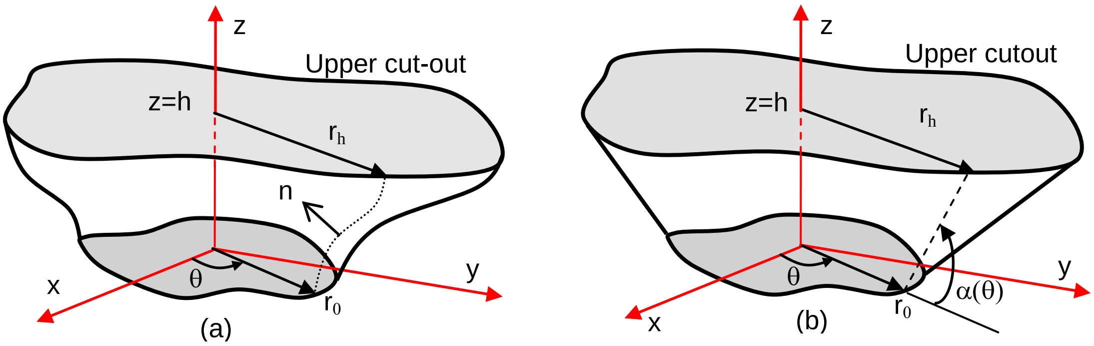

Figure 4. (a) Unconstrained and (b) partially constrained optimum scarf problem

4. A conical optimal solution

With the scarf being given by expression (9), the maximum shear stress and the normal stress can be readily evaluated. It can be shown that the lower cut-out shape needs to satisfy the following relationship to ensure the adhesive failure index be independent of radius *r*,

$$r_0(\theta) = C / \tan\alpha(\theta)\,, \tag{10}$$

where *C* is a constant. In this case, the upper cut-out shape $r_h(\theta)$ is

$$r_h(\theta) = (C + h) / \tan\alpha(\theta)\,. \tag{11}$$

This implies that the optimal scarf is a special conical surface whose apex is located at $z = -C$. The upper cut-out can be viewed as the base of the cone. The optimisation problem now reduces to finding the appropriate cross-section shape, which relates to the scarf angle via equation (10). It is worth noting that the shapes given by the maximum-principal-stress method, the interpolation method, and the radial-stress method are special cases. The scarf surface is

$$Z = r\tan\alpha(\theta) - C\,, \tag{12}$$

The pertinent surface normal is

$$\vec{n} = \frac{(-\cos\theta\sin\alpha + a'\sin\theta\sec\alpha)\vec{i} - (\sin\theta\sin\alpha + a'\cos\theta\sec\alpha)\vec{j} + \cos\alpha\,\vec{k}}{\sqrt{1 + (\alpha')^2\sec^2\alpha}} \tag{13}$$

Since the governing equation for the optimal scarf angle $\alpha(\theta)$ is a highly non-linear differential equation, an iterative approach is adopted, choosing an ellipse as the initial guess for the cross-section shape,

$$(x/a)^2 + (y/b)^2 = 1 \tag{14}$$

where $a = (C + h)/\tan\alpha_0$, and $b = (C + h)/\tan\alpha_{90}$. Here the two scarf angles, α_0 and α_{90} , are given by

$$\alpha_0 = \frac{1}{2}\sin^{-1}\left(\frac{2\tau_Y}{\sigma_x}\right) \tag{15}$$

$$\alpha_{90} = \frac{1}{2}\sin^{-1}\left(\frac{2\tau_Y}{\sigma_y}\right) \tag{16}$$

It can be shown that the scarf surface is given by,

$$Z_1 = r\sqrt{\left(\cos\theta\tan\alpha_0\right)^2 + \left(\sin\theta\tan\alpha_{90}\right)^2} - C = r\tan\alpha_1(\theta) - C\,, \tag{17}$$

with

$$\alpha_1(\theta) = \tan^{-1}\sqrt{\left(\cos\theta\tan\alpha_0\right)^2 + \left(\sin\theta\tan\alpha_{90}\right)^2}\,. \tag{18}$$

With the above expression as the initial guess, first order solution can be obtained by approximating α' with $d\alpha_1/d\theta$. Higher order approximations can be determined by repeating this process.

Numerical calculations revealed the solution converged very quickly, with the error reducing to below 1% after one iteration. This implies that the initial approximation of elliptical cut-out is very close to the optimum solution. In the case of small scarf angle, the ratio of the major to minor axes of the ellipse is equal to

$$\frac{b}{a} \approx \frac{\alpha_0}{\alpha_{90}} \approx \frac{\sigma_y}{\sigma_x} \tag{19}$$

which is identical to the ratio pertinent to a harmonic hole for a uniform biaxial field [6]. One major difference between a harmonic hole and the optimal scarf is that the hoop stress along the edge of a harmonic hole remains constant, whereas the maximum adhesive shear stress on the optimal scarf surface is constant.

The resulting repair geometry and FCI distribution is shown in Figure 5. It can be seen that the elliptical scarf repair with an elliptical cut-out (double-ellipse repair) can be considered to represent an optimum solution. The variation in failure index is far less than for other shapes; this is mainly due to the edge effects which are a characteristic of all scarf repairs without an external doubler.

The scarf angle distributions of all the solutions are compared in Figure 6. It can be seen that the elliptical repair with elliptical cut-out has the highest average α, hence minimising the amount of material removed. However, this is potentially offset by an increase in the cut-out size necessitated to achieve this distribution. Whether the need to craft an elliptical cut-out is disadvantageous or not will ultimately depend on the shape, size and orientation of the initial damage relative to the stress field.

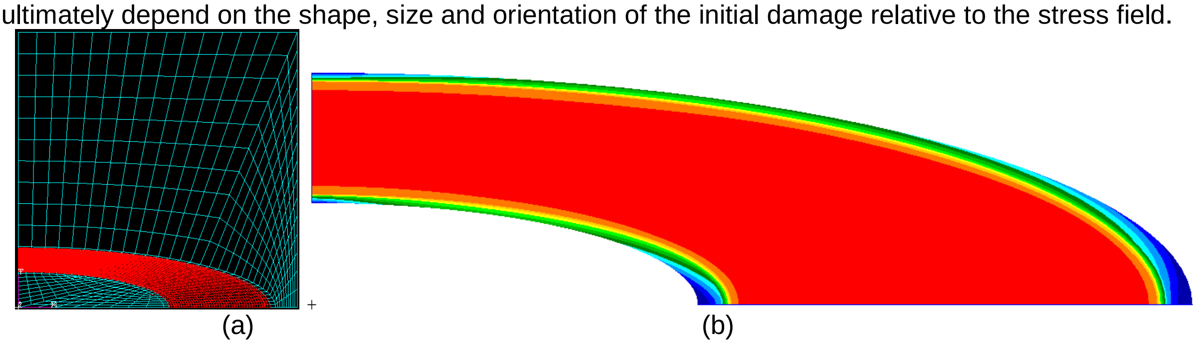

Figure 5. (a) Elliptical scarf with elliptical cutout, (b) resulting FCI (where max. = 1.04, min. = 0.1)

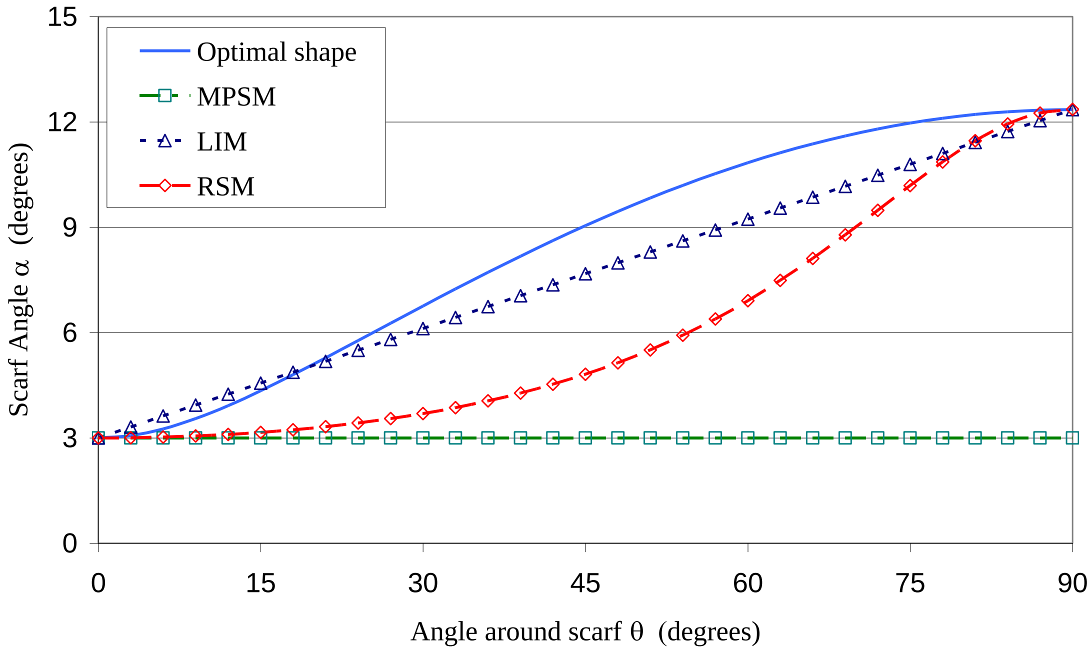

Figure 6. Summary of α versus θ for all examined repair schemes

6. Conclusion

From the exploration of various optimum or near-optimum scarf repair geometries, it can be seen that significant savings can be made to the amount of material removed when adopting an optimum repair over a conventionally-designed repair. This investigation has highlighted the significance of having self-similar repair geometry to avoid local stress concentrations that would be neglected by simple analysis techniques. Future work may investigate alternate methods of tackling the optimisation problem that will allow for more arbitrarily defined geometries. Although some improved geometries have been presented above, an automated optimisation process would prove valuable in the design of repairs for stress states other than biaxial tension. A validated numerical procedure could also be extended to consider multiple load cases. The robustness of the solution and issues surrounding implementation to a real structure will be investigated in subsequent studies.

References

[1] Dutton, S. and Baker, A.A., Aircraft Applications and Design Issues. In J.A. Schetz (Ed.), Composite Materials for Aircraft Structures, 2004, p. 435 – 475. American Institute of Aeronautics and Astronautics: Reston VA.

[2] Harman, A. and Wang C.H., Analytic and finite element stress predictions in two dimensional scarf joints. in Australian International Aerospace Congress (AIAC-11), March 13-17, 2005. Melbourne, Australia.

[3] Gunnion, A.J. and Herszberg. I., Parametric study of scarf joints in composite structures. Composite Structures, 2006. 75(1-4): p. 364–376.

[4] Wang, C.H. and Gunnion, A.J. On the design methodology of scarf repairs to composite laminates, Composites Science and Technology [Article in Press], 2007.

[5] Ojalvo, I.U., Optimization of bonded joints. AIAA Journal, 1985. 23(10): p. 1578-1582.

[6] Bjorkman, G. S. and Richards R. (1976), Harmonic holes – an inverse problem in elasticity, *J. Applied Mechanics*, Vol. 43, 414-418.